In Proceeding of 5th Hellenic Astronomical Conference, Fodele 2001

A symplectic mapping model for the study of 3/4 resonant trans-Neptunian motion and spectral dynamics.

Th. Kotoulas, G. Voyatzis,
and J. Hadjidemetriou
Section of Astrophysics, Astronomy and Mechanics
Department of Physics, University of Thessaloniki,
54006 Thessaloniki, Greece

Abstract

We present a symplectic mapping model that it is valid close to the 3/4 exterior resonance in a Sun-Neptune-EKBO system, for planar motion. The mapping is based on the averaged Hamiltonian close to this resonance. The topology of the mapping is similar to that of the Poincaré map of the real system. Using this model we study the evolution of objects near the 3/4 resonance where both chaotic and regular motions depending on the initial phase of the object are apparent. By using a spectral method, which classifies the trajectories as ordered or chaotic, a large number of trajectories is examined and a clear picture that describes the dynamics in the plane a-e is produced.

1 Introduction

The orbital evolution of EKBOs (Edgeworth Kuiper belt objects) has been recently a topic of intense research [1,4]. In this work we investigate the long term evolution of Kuiper belt objects near 3:4 resonance with Neptune using a four-dimensional symplectic mapping model. Results of the dynamical evolution of the EKBOs near the 3:4 resonance can be taken by the combination of symplectic maps and the method of finding regular and chaotic orbits through the spectral analysis of short-dated time-series.

2 The Basic Model: The restricted three-body problem (3BPR)

2.1 The Circular Case

In this model Neptune revolves around Sun in a circular orbit and the small object moves in the orbital plane of these two bodies. We consider a rotating frame of reference xOy whose x-axis is the line joining Sun with Neptune. In this frame there exist two basic families of symmetric periodic orbits: $I_{3/4}$ & $II_{3/4}$. Along the family $II_{3/4}$ there is a small unstable area around e=0.60 because we are close to a collision orbit. In figure 1a we have drawn the families of periodic orbits at the resonance 3/4 in a diagram x_0-energy constant.The stability is also indicated.

2.2 The Elliptic Case

In this model Neptune revolves around Sun in an elliptic orbit and the small object moves in the orbital plane of these two bodies. There are two families of periodic orbits of the elliptic restricted three body problem that bifurcate from a point with period T=8π; we call them I_e and II_e (figure 1b). Both of them are unstable.

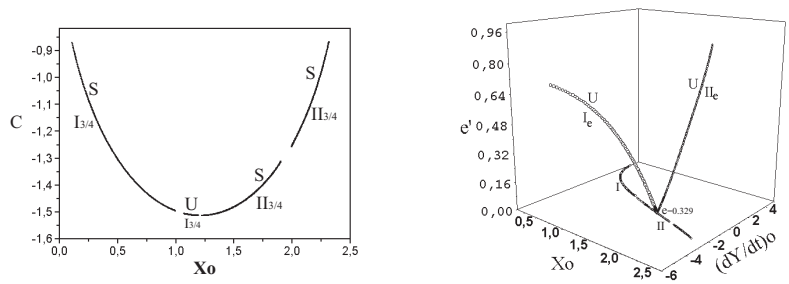

Figure 1: (a) Families of periodic orbits at the circular 3BPR (b)Families of periodic orbits at the elliptic 3BPR. S,U denote the stable and unstable orbits respectively.

2.3 The Mapping Model

The mapping model that we will construct is based on the averaged Hamiltonian of the elliptic restricted problem at 3:4 resonance. The averaged Hamiltonian can be expressed in terms of the resonant action-angle variables S, N, σ, ν :

$$S = \sqrt{a}(1-\sqrt{1-e^2}), N = \sqrt{a}(\frac{3}{4}-\sqrt{1-e^2}), \sigma = -3\lambda'+4\lambda-\varpi, \nu = +3\lambda'-4\lambda+\varpi'$$

where a, e, λ, ϖ are the semimajor axis, the eccentricity, the mean longitude and the longitude of the perihelion of the test particle and the corresponding primed quantities refer to Neptune. In these variables, the averaged Hamiltonian of the elliptic restricted three body problem is [6]

$$\hat{H} = H_0(S, N) + \mu H_1(\sigma, S, N) + \mu e' H_2(\sigma, S, \nu, N)$$

We construct a symplectic mapping model [3] using the generating function

$$W = S_{n+1}\sigma_n + N_{n+1}\nu_n + T \cdot H''(S_{n+1}, \sigma_n, N_{n+1}, \nu_n) \tag{1}$$

through the equations:

$$\sigma_{n+1} = \frac{\partial W}{\partial S_{n+1}}\ ,\ S_n = \frac{\partial W}{\partial \sigma_n}\ ,\ \nu_{n+1} = \frac{\partial W}{\partial N_{n+1}}\ ,\ N_n = \frac{\partial W}{\partial \nu_n} \tag{2}$$

where T=8π is the synodic period of a 3:4 resonant periodic orbit. The new "corrected" averaged Hamiltonian is given by:

$$H'' = H_0(S, N) + \mu H_1'(\sigma, S, N) + \mu e' H_2(\sigma, S, \nu, N) + H_{cor1}(N) + H_{cor2}(\nu)$$

where $H_1' = -\{eA_{11}\cos\sigma + e^2(A_{20} + qA_{22}\cos 2\sigma) + e^3(A_{31}\cos\sigma + qA_{33}\cos 3\sigma)\}$ and $H_{cor1} = C_{11}N^2 + C_{12}N, H_{cor2} = -\mu e'(B_{31}\cos\nu + B_{32}\cos 2\nu)$. The correction factor q that was introduced in the constants A_{22} and A_{33} is used to correct the stability of the mapping's fixed points. The values of the constants are empirically found: $q = 0.05, C_{11} = -0.0052, C_{12} = -0.002650, B_{31} = -5.5, B_{32} = 1.15$.

3 Evolution of an EKBO close to the 3/4 Resonance

In order to study the dynamics of 3/4 resonant Kuiper belt objects, we use the four-dimensional map to integrate planar orbits for 10^8 years. In figures 2a-2c and 3a-3c we present samples of regular and chaotic orbits at the 3/4 resonance. Also, we tested the behavior of critical angles σ and ν_8=-(σ+ν). The transition of the behavior of an orbit from regular to chaotic is characterized by a conversion of the σ-libration to circulation.

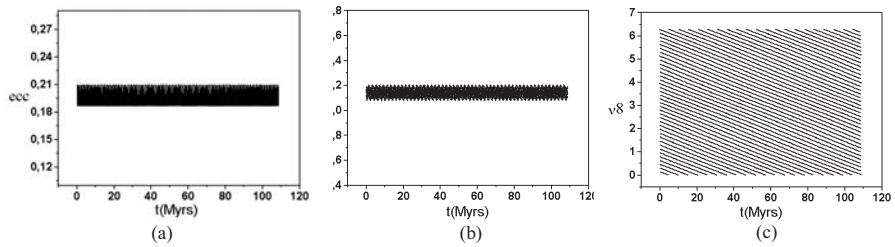

Figure 2: Time evolution for a_0=36.415A.U., e_0=0.21, $\sigma_0 = \nu_0 = \pi$, of the a) eccentricity b) angle σ and c) angle ν_8.

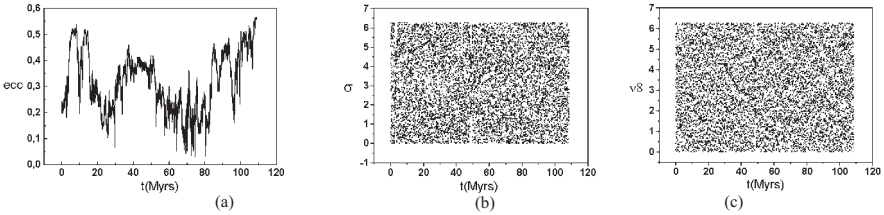

Figure 3: Time evolution for a_0=36.415 A.U., e_0=0.21, $\sigma_0 = 0$ and $\nu_0 = \pi$ of the a) eccentricity b) angle σ and c) angle ν_8.

4 Spectral maps and phase space dynamics

Let $F = F(S, N)$, where S, N are the resonant actions, be an integral of H_0. Under the effect of the perturbation μH_1 , F varies with the time along an orbit; so $F = F(t)$. Let $P(f)$ be the spectral density of the $F(t)$ for the time interval [0,T_0], $T_0 >> 1$. If $F(t)$ is computed along an orbit which is on an invariant torus, then $P(f) < \frac{\gamma}{f}\exp(\frac{-\alpha}{f^\kappa})$, for $f \in (0, f_0)$, $f_0 = O(\epsilon))$ where γ, κ, α are positive constants [7]. Then, for regular orbits, $P(f) \to 0$ as $f \to 0$, while, for chaotic orbits, $P(f)$ tends to a positive nonzero value or diverges as noise $\frac{1}{f}$, as $f \to 0$. Actually, the spectral density is computed using discrete Fourier transform (DFT) on a discrete time-series $F_i = F(i \cdot \Delta t)$, $i = 1, ..., 2N$, giving a discrete function of spectral density $P_i = P(f_i)$, $i = 1, 2, ..., N$ and the existence or not of important spectral lines at low frequencies can be estimated with the indicator of "low band power" $\beta_{(K)} < 0$ that is defined as following: $\beta_{(K)} = \log(\sum_{i=1}^{K} P_i) - \log \overline{P}$, where $0 < K << N$. Generally, by considering threshold values b_o and b_c (typically β_o =-10, β_c=-5), we can separate $\beta_{(K)} - levels$ into three regions:

- (i) $\beta_{(K)} < \beta_o$: regular orbits,
- ii)$\beta_o < \beta_{(K)} < \beta_c$: weak chaotic orbits or strongly perturbed (but still) regular orbits,
- (iii)$\beta_{(K)} > \beta_c$: chaotic orbits

In the 4-D mapping space, formed by the variables S, N, σ and ν, we define 2-D surfaces e.g. the surface $\{(a(S, N), e(S, N)), \sigma = \sigma_0, \nu = \nu_0\}$. Each point of the above surfaces corresponds to a point of the phase space and the character of the orbit that represents is given by the indicator $\beta_{(K)}$. We construct lattices 100×100 and we calculate $\beta_{(16)}$ for time-series of 262144 iterations of the mapping corresponding to 43.2 Myrs.

In fig.4a (circular case) a very large stable region around a=36.415 A.U. appears. In fig.4b (elliptic case) the stable area around a=36.415 A.U. shrinks. In these cases $\sigma_0 = \pi, \nu_0 = \pi$. In fig.4c we give a map $(\sigma - e)$ for the elliptic planar problem and for a=36.415A.U., $\nu = \pi$. For low eccentricities, stable orbits exist between $\sigma \approx 2\pi/3$ and $\sigma \approx 3\pi/2$. Increasing the value of eccentricity this region weakens.

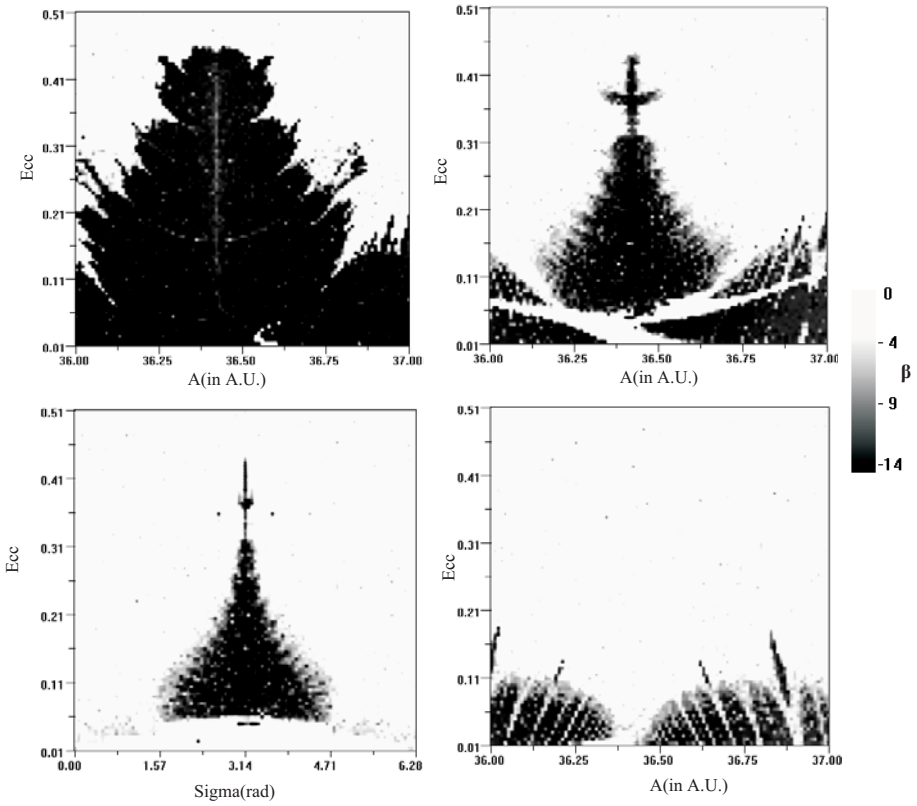

Figure 4: Map (a-e) for a) the Circular 3BPR b) the Elliptic 3BPR c)Map $(\sigma - e)$at a=36.415 A.U. d) Map (a-e) for $\sigma_0 = 0$

For $\sigma = 0$, almost all the regions around the resonance become unstable(fig. 4d). In this case EKBOs are not protected from phase and their orbits are strongly chaotic becoming Neptune-crossers.

References

[1] Duncan M., Levinson H.F. & Budd S.M.(1995), The dynamical structure of the kuiper Belt, Astron. J. **110**, 3073-3081

[2] Ferraz-Mello, S. (1997), A Symplectic Mapping approach to the study of the Stochasticity of asteroidal resonances, Cel.Mech. **65**,421-437

[3] Hadjidemetriou, J.D. (1993), Asteroid motion near the 3:1 Resonance, Cel.Mech. **56**, 563-599

[4] Melita, M.D. and Brunini, A. (2000), Comparative Study of Mean-Motion Resonances in the trans-Neptunian Region, Icarus **147**, 205-219

[5] Sidlichovsky, M. (1992), Mapping For the Asteroidal Resonances, Aston.Astrophys. **259**, 341-348

[6] Sidlichovsky, M. (2000), personal communication

[7] Voyatzis, G. and Ichtiaroglou, S. (1992), On the spectral analysis of trajectories in Hamiltonian systems, J.Phys.A:Math. Gen, **25**, 5931-5943.